Available online at www.eccomasproceedia.org
Eccomas Proceedia UNCECOMP (2023) 48-66

ECCOMAS
Proceedia

UNCECOMP 2023
5th ECCOMAS Thematic Conference on
Uncertainty Quantification in Computational Science and Engineering
M. Papadrakakis, V. Papadopoulos, G. Stefanou (eds.)
Athens, Greece, 12-14 June 2023

BAYESIAN UPDATING OF GLOBAL RESPONSE SENSITIVITY INDICES IN AN INSTRUMENTED STRUCTURE

Bibhas Paul [1], Nisha A S [1], and C S Manohar [2]

[1] Research scholar,
Dept. of Civil Engineering, Indian Institute of Science, Bangalore 5600 12
{bibhaspaul, nishaas}@iisc.ac.in

[2] Professor,
Dept. of Civil Engineering, Indian Institute of Science, Bangalore 5600 12
manohar@iisc.ac.in

Abstract

The study discusses updating the global response sensitivity indices (GRSI) of an instrumented structure by employing factor mapping method in conjunction with an implicit Bayesian framework for combined state and parameter estimation. In conventional factor mapping-based approaches, an ensemble of structural parameters are classified into two disjoint sets, depending on whether a sample vector produces a response in a predefined range of interest or not. A probabilistic distance between the samples, thus classified, is measured for each parameter or group of parameters. In this study, we use Bhattacharyya's distance as the probabilistic distance measure to determine the sensitivity of the associated individual parameters or groups of parameters. The estimation of this distance requires the probability density functions (pdfs) of the underlying random variables. This in turn allows one to employ the posterior pdfs of parameters in computing Bhattacharya's distance-based GRSI. These posterior pdfs are obtained from the combined state and parameter estimation problem, which ensures the assimilation of the measurement data while computing the GRSI values. In this study, the developed method of updating GRSI has been demonstrated on a five-storied, bending-torsion coupled, instrumented building frame subject to a scaled recorded ground motion. An application of GRSI in the context of structural engineering problems, specifically for model reduction is also discussed.

Keywords: Global response sensitivity analysis, Bayesian framework, implicit Kalman filter, MCMC, factor mapping, Bhattacharyya's distance

ISSN:2623-3339
Peer-review under responsibility of the organizing committee of UNCECOMP 2023.
doi: 10.7712/120223.10324.19770

1 INTRODUCTION

The methods of global response sensitivity analysis (GRSA) offer powerful tools in the study of randomly parametered and/or randomly excited engineering systems. These tools aim to establish the relative importance of underlying random variables in terms of their contributions to the variability in a chosen response quantity of interest. The importance measures thus determined are valuable in probabilistic model reduction and in planning experiments to collect data on underlying random quantities. Several methods exist to achieve these goals, including those based on Sobol's decomposition [1], probabilistic model distance measures [2], and factor mapping method [3,4]. To the best of the authors' knowledge, the available studies focus on performing GRSA on mathematical models of engineering systems, and hardly any study focuses on GRSA as applied to instrumented existing structures. The proposed study aims to remedy this situation. Accordingly, we consider the problem of updating global response sensitivity indices (GRSI) of a numerically stiff, instrumented, linear building frame subject to earthquake-induced dynamic loads based on the measured response of the system. The problem is formulated within the Bayesian state and parameter estimation framework based on implicit state space models [5]. The steps involved in the study are as follows:

Step-1 Prior model for the GRSI: Here, we consider a finite element model for the building frame and treat the system parameters (encompassing, stiffness, damping, and mass properties) as a set of non-Gaussian dependent random variables. We employ the factor mapping method to estimate the GRSI with respect to individual or groups of random variables [6].

Step-2 Combined state and parameter estimation: Here, we combine implicit Kalman filter tools for state estimation [5] and MCMC-based sampling schemes for parameter estimation. The prior models for system parameters are taken to coincide with those used in Step 1. This results in an ensemble of samples for the system parameters and response quantities of interest from which the posterior probability density functions for these quantities can be estimated.

Step-3 Updating of the GRSI. Here, we employ the samples from the posterior pdfs of identified system parameters and response quantities of interest within the framework of the factor mapping method and arrive at the updated estimates for the GRSI.

The proposed framework is illustrated based on experimental data on a bending torsion coupled five-storied building frame model tested on a multi-axes earthquake shake table. The prior GRSI values and posterior GRSI values are computed and compared. Also, the question on model reductions based on GRSI values of the parameters is addressed.

2 PROBLEM STATEMENT

Consider a five-storied, bending-torsion coupled, building frame subjected to a scaled recorded ground excitation, such that the response of the frame remains within the elastic regime. A 15 degrees of freedom (DOFs) model is derived with each floor having two translational and one rotational degrees of freedom. The governing equation of motion is given as

$$\mathbf{M}(\boldsymbol{\Theta})\ddot{\boldsymbol{X}}(t)+\mathbf{C}(\boldsymbol{\Theta})\dot{\boldsymbol{X}}(t)+\mathbf{K}(\boldsymbol{\Theta})\boldsymbol{X}(t)=-\mathbf{M}(\boldsymbol{\Theta})\boldsymbol{L}\ddot{u}_g(t)+\boldsymbol{\xi}(t),\boldsymbol{X}(0)=\dot{\boldsymbol{X}}(0)=\mathbf{0} \qquad (1)$$

where $\mathbf{M}(\boldsymbol{\Theta})$, $\mathbf{C}(\boldsymbol{\Theta})$, and $\mathbf{K}(\boldsymbol{\Theta})$ are mass, damping, and stiffness matrices respectively, $\boldsymbol{\Theta}\in\mathbb{R}^n$, denotes a vector random variable, that contains the uncertain system parameters, $\ddot{u}_g(t)$ is the ground acceleration, $\boldsymbol{L}$ is the influence vector, and $\boldsymbol{\xi}(t)$ is a vector random pro-

cess that models the imperfections in formulating the mathematical model and the errors associated with the measurement of the forcing function. Here, we have considered Rayleigh's proportional damping model, $\mathbf{C} = \alpha_1 \mathbf{M} + \alpha_2 \mathbf{K}$. For the current study, mass matrix $\mathbf{M}$ is treated as deterministic, while the components of the stiffness matrix and damping ratios are treated as a set of dependent and non-Gaussian random variables. The performance of the building frame is characterized in terms of three response measures, namely (1) maximum inter-story drift ratio (PM_1), (2) maximum inter-story rotation (PM_2), and (3) maximum base shear (PM_3), given by

$$\begin{aligned} PM_1 &= \max_{1\le i\le N_f} \max_{0<t<\infty} \left(\left| \frac{\Delta_i^x(t) - \Delta_{i-1}^x(t)}{h_i} \right|, \left| \frac{\Delta_i^y(t) - \Delta_{i-1}^y(t)}{h_i} \right| \right) \\ PM_2 &= \max_{1\le i\le N_f} \max_{0<t<\infty} \left| \varphi_i(t) - \varphi_{i-1}(t) \right| \\ PM_3 &= \max_{0<t<\infty} \left(\left| k_1 \Delta_1^x + c_1 \dot{\Delta}_1^x \right|, \left| k_1 \Delta_1^y + c_1 \dot{\Delta}_1^y \right| \right) \end{aligned} \tag{2}$$

Here, $\Delta_i^x(t), \Delta_i^y(t)$ are two orthogonal components of the translational motion of the i^{th} floor, $\varphi_i(t)$ represents the rotational motion of the i^{th} floor, h_i represents the height of the i^{th} story, k_1 represents the combined stiffness of all columns at 1st story level, c_1 represents damping constant associated with the 1st story level, and N_f indicates the number of floors in the frame. The samples of the response function, $PM = f(\boldsymbol{\Theta})$ are obtained using equation (2) for each realization of $\boldsymbol{\Theta}$, generated using Monte Carlo simulations. Here, the response function PM could be any predefined candidate response from $\{PM_1, PM_2, PM_3\}$. The problem on hand is to perform the global response sensitivity analysis of an instrumented structure based on implicit state space models with respect to uncertain system parameters or their various groups. This requires defining a reference set A, such that $A = [a \le PM \le b]$ encompasses the region of interest of the response quantity. We consider m disjoint groups formed from the components of the parameter vector $\boldsymbol{\Theta}$, such that, $\boldsymbol{\Theta} = \left[\boldsymbol{\Theta}^1 \;\; \boldsymbol{\Theta}^2 \;\; \cdots \;\; \boldsymbol{\Theta}^m \right]$, and $n_1 + n_2 + \cdots + n_m = n$; n_j, the number of components in j^{th} group. We then classify the samples of $\boldsymbol{\Theta}$ into two sets $\theta_A = \left[\theta_A^1 \;\; \theta_A^2 \;\; \cdots \;\; \theta_A^m \right]$, and $\theta_{A^c} = \left[\theta_{A^c}^1 \;\; \theta_{A^c}^2 \;\; \cdots \;\; \theta_{A^c}^m \right]$, such that $\theta_A = \left\{ \theta \middle| f(\theta) \in A \right\}$ and $\theta_{A^c} = \left\{ \theta \middle| f(\theta) \in A^c \right\}$. A measure of sensitivity of PM with respect to the group $\boldsymbol{\Theta}^j$ is defined as $d_j = \text{dist}\left(\boldsymbol{\Theta}_A^j, \boldsymbol{\Theta}_{A^c}^j \right)$, which is often termed as global response sensitivity index (GRSI) associated with group $\boldsymbol{\Theta}^j$. Here the samples contained in θ_A^j and $\theta_{A^c}^j$ are assumed to be generated from two n_j dimensional multivariate pdf-s of non-Gaussian random variables $\boldsymbol{\Theta}_A^j$ and $\boldsymbol{\Theta}_{A^c}^j$. These two multivariate pdfs, $p_{\boldsymbol{\Theta}_A^j}(\boldsymbol{u})$ and $p_{\boldsymbol{\Theta}_{A^c}^j}(\boldsymbol{u})$ are not known in closed form expression, but the samples from these pdfs are available in θ_A^j and $\theta_{A^c}^j$. Here $\text{dist}(\bullet, \bullet)$ is a legitimate distance metric between two random variables. In this study, we consider Bhattacharyya's distance [7] to estimate $d_j = \text{dist}\left(\boldsymbol{\Theta}_A^j, \boldsymbol{\Theta}_{A^c}^j \right)$, which is defined as,

$$d_j = -\ln \rho_j; \text{ where } \rho_j = \int_{\Omega} \sqrt{p_{\boldsymbol{\Theta}_A^j}(\boldsymbol{u}) \, p_{\boldsymbol{\Theta}_{A^c}^j}(\boldsymbol{u})} d\boldsymbol{u} \; ; \; j = 1, 2 \ldots, m \tag{3}$$

The integral in equation (3) is evaluated using Monte Carlo integration technique, given by

$$\rho_j = \int_{\Omega} \sqrt{p_{\boldsymbol{\Theta}_{\mathrm{A}}^j}(\boldsymbol{u})\, p_{\boldsymbol{\Theta}_{\mathrm{A}^c}^j}(\boldsymbol{u})}\, d\boldsymbol{u} = \int_{\Omega} \sqrt{\frac{p_{\boldsymbol{\Theta}_{\mathrm{A}}^j}(\boldsymbol{u})}{p_{\boldsymbol{\Theta}_{\mathrm{A}^c}^j}(\boldsymbol{u})}}\, p_Y(\boldsymbol{u})\, d\boldsymbol{u} = \mathrm{E}_{p_{\boldsymbol{\Theta}_{\mathrm{A}^c}^j}}\left[\sqrt{\frac{p_{\boldsymbol{\Theta}_{\mathrm{A}}^j}(\boldsymbol{U})}{p_{\boldsymbol{\Theta}_{\mathrm{A}^c}^j}(\boldsymbol{U})}}\right] = \frac{1}{N(\boldsymbol{\Theta}_{A^c})} \sum_{k=1}^{N(\boldsymbol{\Theta}_{A^c})} \sqrt{\frac{p_{\boldsymbol{\Theta}_{\mathrm{A}}^j}(\boldsymbol{u}^{(k)})}{p_{\boldsymbol{\Theta}_{\mathrm{A}^c}^j}(\boldsymbol{u}^{(k)})}} \tag{4}$$

Here $N(\boldsymbol{\Theta}_{A^c})$ is the number of samples in $\boldsymbol{\Theta}_{A^c}$ and $N(\boldsymbol{\Theta}_A) + N(\boldsymbol{\Theta}_{A^c}) = N$, where N is the number of Monte Carlo samples used. The multivariate pdfs $p_{\boldsymbol{\Theta}_{\mathrm{A}}^j}(\boldsymbol{u})$ and $p_{\boldsymbol{\Theta}_{\mathrm{A}^c}^j}(\boldsymbol{u})$ in equation (4), which are in general non-gaussian in nature are to be approximated. Estimation of joint pdf-s employing a normalized histogram approach, which works well for low dimensional random vectors, becomes infeasible as the dimension of the random vector increases [8]. To circumvent this problem, we apply Nataf's model-based approximation [9] for the joint pdf-s involved in equation (4), which is recently developed by the authors [6]. As the expression of Bhattacharyya's distance involves the joint pdf-s of the system parameters $\boldsymbol{\Theta}$, it offers a strategy to update the global response sensitivity indices, by employing posterior joint pdfs of the system parameters $p_{\boldsymbol{\Theta}|D}(\theta|D)$ instead of $p_{\boldsymbol{\Theta}}(\theta)$. Here, D is the measurement data. Thus, the updated GRSI can be obtained as,

$$\tilde{d}_j = -\ln \tilde{\rho}_j;\ \text{where}\ \tilde{\rho}_j = \int_{\Omega} \sqrt{p_{\boldsymbol{\Theta}_{\mathrm{A}}^j|D}(\boldsymbol{u}|D)\, p_{\boldsymbol{\Theta}_{\mathrm{A}^c}^j|D}(\boldsymbol{u}|D)}\, d\boldsymbol{u}\ ;\ j = 1,2\ldots,m \tag{5}$$

where posterior pdf-s are obtained, in general, using Bayes' theorem [10] given by

$$p_{\boldsymbol{\Theta}_{\mathrm{A}}^j|D}(\boldsymbol{u}|D) = c_1 p_{D|\boldsymbol{\Theta}_{\mathrm{A}}^j}(D|\boldsymbol{u})\, p_{\boldsymbol{\Theta}_{\mathrm{A}}^j}(\boldsymbol{u}),\ \text{and,}\ p_{\boldsymbol{\Theta}_{\mathrm{A}^c}^j|D}(\boldsymbol{u}|D) = c_2 p_{D|\boldsymbol{\Theta}_{\mathrm{A}^c}^j}(D|\boldsymbol{u})\, p_{\boldsymbol{\Theta}_{\mathrm{A}^c}^j}(\boldsymbol{u}) \tag{6}$$

To the best of the authors' knowledge, studies available on global response sensitivity analysis mostly focus on performing GRSA on mathematical models of engineering systems, and hardly any study available focusing on GRSA applied to existing instrumented structures, or updating the GRSI, as measurement data become available in an instrumented system. Therefore, updating of GRSI conditioned on measurement in an instrumented structure sets the novelty of this study. Section 3 focuses on the GRSA employing Bhattacharyya's distance-based factor mapping method applied to a mathematical model and section 4 focuses on the estimation of posterior joint pdfs in an instrumented system under the framework of combined state and parameter estimation based on implicit state space models.

3 BHATTACHARYYA'S DISTANCE-BASED GLOBAL RESPONSE SENSITIVITY ANALYSIS

In the preceding section, we developed an estimator to evaluate the multi-fold integration in parameter space in equation (3). We still need to approximate the joint pdf-s, $p_{\boldsymbol{\Theta}_{\mathrm{A}}^j}(\boldsymbol{u})$ and $p_{\boldsymbol{\Theta}_{\mathrm{A}^c}^j}(\boldsymbol{u})$ from the available samples $\boldsymbol{\theta}_A^j$ and $\boldsymbol{\theta}_{A^c}^j$. For the sake of simplicity of notations, we consider a $r \times 1$ vector of random variables, $\boldsymbol{U}$, for which the associated joint pdf $p_{\boldsymbol{U}}(\boldsymbol{u})$ is not known; instead, we have simulated data, $\left\{\boldsymbol{u}^{(k)}\right\}_{k=1}^{N_U} \sim p_{\boldsymbol{U}}(\boldsymbol{u})$. The objective here is to estimate the joint pdf $p_{\boldsymbol{U}}(\boldsymbol{u})$ as a function of data $\left\{\boldsymbol{u}^{(k)}\right\}_{k=1}^{N_U}$. The steps involved in estimating the joint pdf based on available samples are discussed as follows:

1. From the samples of each component of $\boldsymbol{U} = \left[U_1 \quad U_2 \quad \ldots \quad U_r\right]^{\mathrm{t}}$, estimate the 1st order pdf $\hat{p}_{U_i}(u_i);\ i = 1,2,\ldots,r$ by employing a normalized histogram approach, i.e., normal-

izing the ordinate of the histogram generated using data $\left\{u_i^{(k)}\right\}_{k=1}^{N_U}$, such that area under the histogram becomes unity.

2. Next, estimate the 1st order CDFs, $\hat{F}_{U_i}(u_i);\ i=1,2,\ldots,r$, for each component of $\boldsymbol{U}=\left[U_1 \quad U_2 \quad \ldots \quad U_r\right]^{\mathrm{t}}$ by rank ordering the samples $\left\{u_i^{(k)}\right\}_{k=1}^{N_U}$ in ascending order.

3. Next, we introduce an iso-probabilistic transformation $\hat{F}_{U_i}(u_i)=\Phi(\varsigma_i);\ i=1,2,\ldots,r$. Here, ς_i is a standard normal random variable and $\Phi(\bullet)$ is the CDF of a standard normal random variable. Obtain the samples of ς_i from the samples, $\left\{u_i^{(k)}\right\}_{k=1}^{N_U}$, using the relation $\varsigma_i=\Phi^{-1}\hat{F}_{U_i}(u_i);\ i=1,2,\ldots,r$.

4. Estimate the covariance matrix $\boldsymbol{\Sigma}_{\boldsymbol{\varsigma}}$ of the random vector $\boldsymbol{\varsigma}=\left[\varsigma_1 \quad \varsigma_2 \quad \ldots \quad \varsigma_r\right]^{\mathrm{t}}$. This is essentially a matrix of correlation coefficients among the components of $\boldsymbol{\varsigma}=\left[\varsigma_1 \quad \varsigma_2 \quad \ldots \quad \varsigma_r\right]^{\mathrm{t}}$, with diagonal entries as unity.

5. Now, applying Nataf's model, the joint pdf of the random vector $\boldsymbol{U}$ can be approximated as,

$$\hat{p}_U(\boldsymbol{u})=\phi_r\left(\left[\varsigma_1 \quad \varsigma_2 \quad \ldots \quad \varsigma_r\right]^{\mathrm{t}};\mathbf{0},\boldsymbol{\Sigma}_{\boldsymbol{\varsigma}}\right)\frac{\prod_{i=1}^{r}\hat{p}_{U_i}(u_i)}{\prod_{i=1}^{r}\phi(\varsigma_i;0,1)} \tag{7}$$

Here, $\phi_r\left(\bullet;\mathbf{0},\boldsymbol{\Sigma}_{\boldsymbol{\varsigma}}\right)$ denotes an r-dimensional Gaussian pdf with the mean vector as zero and covariance $\boldsymbol{\Sigma}_{\boldsymbol{\varsigma}}$. $\phi(\bullet;0,1)$ denotes a 1st order pdf of a standard normal random variable. Following steps 1-5, now, we can estimate the joint pdfs of the random variables $\boldsymbol{\theta}_A^j$, and, $\boldsymbol{\theta}_{A^c}^j$ based on their available samples and further, plugging the estimated joint pdfs in equation (4), we can estimate the Bhattacharyya coefficient, ρ_j, as follows:

$$\begin{aligned}\hat{\rho}_j &= \frac{1}{N\left(\boldsymbol{\Theta}_{A^c}\right)}\sum_{k=1}^{N\left(\boldsymbol{\theta}_{A^c}\right)}\sqrt{\frac{\hat{p}_{\boldsymbol{\theta}_A^j}\left(\boldsymbol{u}^{(k)}\right)}{\hat{p}_{\boldsymbol{\theta}_{A^c}^j}\left(\boldsymbol{u}^{(k)}\right)}} \\ &= \frac{1}{N\left(\boldsymbol{\Theta}_{A^c}\right)}\sum_{k=1}^{N\left(\boldsymbol{\theta}_{A^c}\right)}\sqrt{\frac{\phi_r\left(\left[\Phi^{-1}\hat{F}_{U_1}\left(u_1^{(k)}\right) \quad \Phi^{-1}\hat{F}_{U_2}\left(u_2^{(k)}\right) \quad \ldots \quad \Phi^{-1}\hat{F}_{U_r}\left(u_r^{(k)}\right)\right]^{\mathrm{t}};\mathbf{0},\boldsymbol{\Sigma}_{\boldsymbol{\varsigma}(V)}\right)\dfrac{\prod_{i=1}^{r}\hat{p}_{V_i}\left(u_i^{(k)}\right)}{\prod_{i=1}^{r}\phi\left(\Phi^{-1}\hat{F}_{V_i}\left(u_i^{(k)}\right);0,1\right)}}{\phi_r\left(\left[\Phi^{-1}\hat{F}_{U_1}\left(u_1^{(k)}\right) \quad \Phi^{-1}\hat{F}_{U_2}\left(u_2^{(k)}\right) \quad \ldots \quad \Phi^{-1}\hat{F}_{U_r}\left(u_r^{(k)}\right)\right]^{\mathrm{t}};\mathbf{0},\boldsymbol{\Sigma}_{\boldsymbol{\varsigma}(U)}\right)\dfrac{\prod_{i=1}^{r}\hat{p}_{U_i}\left(u_i^{(k)}\right)}{\prod_{i=1}^{r}\phi\left(\Phi^{-1}\hat{F}_{U_i}\left(u_i^{(k)}\right);0,1\right)}}}\end{aligned} \tag{8}$$

Here, $\left\{u_i^{(k)}\right\}_{k=1}^{N_U}\sim p_{U_i}(\boldsymbol{u}_i)$. Again, for the simplicity of notation, we consider the vector random variables $\boldsymbol{\theta}_{A^c}^j$, and, $\boldsymbol{\theta}_A^j$ as $\boldsymbol{U}$, and, $\boldsymbol{V}$ in the above expressions.

6. Finally, one gets the estimator for the Bhattacharyya's distance (or the GRSI associated with the group Θ^j), $\hat{d}_j = -\ln \hat{\rho}_j$.

Remarks:

a. In the approximation of joint pdfs using Nataf's model, we consider the information upto 2nd central moment (covariance) of the component random variables. Higher order moments information can be retained while approximating the joint pdfs using Copula based pdf model [11] or independent component analysis-based approaches [12]. However, these approaches are not discussed in this study.
b. While evaluating Bhattacharyya's coefficient $\hat{\rho}_j$ using the samples, $\left\{u_i^{(k)}\right\}_{k=1}^{N_U}$, one may notice that $\hat{p}_{U_i}\left(u_i^{(k)}\right)$ values are readily available, as the samples $\left\{u_i^{(k)}\right\}_{k=1}^{N_U}$ are realized from the density function $\hat{p}_{U_i}\left(u_i^{(k)}\right)$. One may need to employ a suitable interpolation scheme to determine $\hat{p}_{V_i}\left(u_i^{(k)}\right)$. If $u_i^{(k)}$ lies outside the domain of V_i, then $\hat{p}_{V_i}\left(u_i^{(k)}\right)$ should be taken as zero.
c. For the cases, where GRSI values are sought with respect to individual system parameters, $\Theta_i;\ i = 1,2,\ldots,n$, the problem reduces to estimating Bhattacharyya's distance between two univariate pdfs. Thus, the integration in equation (4) becomes a one-dimensional integration, involving 1st order pdf of $\left(\Theta_A\right)_i$ and $\left(\Theta_{A^c}\right)_i$. Here, Θ_A and Θ_{A^c} are the underlying vector random variables for the samples $\theta_A = \left\{\theta \middle| f(\theta) \in A\right\}$ and $\theta_{A^c} = \left\{\theta \middle| f(\theta) \in A^c\right\}$. In these cases, we do not require to estimate any joint pdf through Nataf's model, that makes the estimation of Bhattacharyya's coefficient, and subsequently Bhattacharyya's distance straightforward.

4 COMBINED STATE AND PARAMETER ESTIMATION USING BAYESIAN FRAMEWORK BASED ON IMPLICIT STATE SPACE MODELS

To proceed further, we interpret equation (1) as an Ito's stochastic differential equation. The frame under consideration exhibits numerical stiff behaviour and hence preferably discretized using the order 1.5 strong Ito's implicit numerical integration scheme [13], leading to the process equation of the form,

$$\boldsymbol{y}_{k+1} = \mathbf{G}_{k+1}(\Theta)\,\boldsymbol{y}_{k+1} + \mathbf{F}_k(\Theta)\,\boldsymbol{y}_k + \boldsymbol{H}_k(\Theta) + \mathbf{Q}_k(\Theta)\,\boldsymbol{w}_k;\ k = 0,1,2,\cdots \tag{9}$$

Here $\mathbf{F}_k(\Theta)$ and $\mathbf{G}_{k+1}(\Theta)$ are $N_x \times N_x$ matrices, the vector $\boldsymbol{H}_k(\Theta)$ of size $N_x \times 1$ represents the applied external excitations, $\mathbf{Q}_k(\Theta)$ is the coefficient matrix of process noise of size $N_x \times N_w$, and $\boldsymbol{w}_k$ is the process noise vector of size $N_w \times 1$ with $\mathrm{E}\left[\boldsymbol{w}_k\right] = 0$ and $\mathrm{E}\left[\boldsymbol{w}_k \boldsymbol{w}_l^{\mathrm{t}}\right] = \delta_{kl} \sum_{w_k}, k,l = 0,1,2,\cdots$. Furthermore, it is assumed that the system is instrumented with a set of N_s number of sensors leading to the measurement equation of the form given by,

$$\boldsymbol{z}_k = \mathbf{h}_k(\Theta)\,\boldsymbol{y}_k + \mathbf{R}_k(\Theta)\,\boldsymbol{v}_k;\ k = 1,2,\cdots,N_T \tag{10}$$

where $\boldsymbol{z}_k$ is the $N_s \times 1$ vector of measurements, $k = 1, 2, \cdots, N_T$ are the discrete-time instants at which measurements are recorded, $\mathbf{h}_k(\Theta)$ is the $N_s \times N_x$ matrix that relates the sensor outputs to the system state vector $\boldsymbol{y}_k$, $\boldsymbol{\nu}_k; k = 1, 2, \cdots, N_T$ is a sequence of independent vector random variables with $\mathrm{E}[\boldsymbol{\nu}_k] = 0$, $\mathrm{E}\left[\boldsymbol{\nu}_k \boldsymbol{\nu}_l^{\mathrm{t}}\right] = \delta_{kl} \boldsymbol{\Sigma}_{\boldsymbol{\nu}_k}, k, l = 1, 2, \cdots N_T$, and $\mathbf{R}_k(\Theta)$ is the $N_s \times N_s$ coefficient matrix of the measurement noise. It is assumed that the forcing vector $\boldsymbol{u}(t)$ is measured. Also, it is assumed that the vectors $\boldsymbol{\nu}_k, k = 1, 2, \cdots, N_T$, the initial condition vector $\boldsymbol{X}_0$, and the noise process $\mathrm{d}\boldsymbol{B}(t)$ are independent. The measurement equation here is taken to be linear. Equations (9) and (10) together constitute the linear dynamic state space model for the combined state and parameter estimation problem. The aim is to estimate the filtering pdf $p(\boldsymbol{y}_k, \Theta | \mathbf{z}_{1:k})$ from which we deduce $p(\boldsymbol{y}_k | \mathbf{z}_{1:k})$ and $p(\Theta | \mathbf{z}_{1:k})$, and the associated moments of interest given by

$$
\begin{aligned}
p(\boldsymbol{y}_k | \mathbf{z}_{1:k}) &= \int p(\boldsymbol{y}_k, \Theta | \mathbf{z}_{1:k}) \, \mathrm{d}\Theta \\
\boldsymbol{a}_{k|k} &= \int\int \boldsymbol{y}_k \, p(\boldsymbol{y}_k, \Theta | \mathbf{z}_{1:k}) \, \mathrm{d}\boldsymbol{y}_k \, \mathrm{d}\Theta \\
\boldsymbol{\Sigma}_{k|k} &= \int\int (\boldsymbol{y}_k - \boldsymbol{a}_{k|k})(\boldsymbol{y}_k - \boldsymbol{a}_{k|k})^{\mathrm{t}} \, p(\boldsymbol{y}_k, \Theta | \mathbf{z}_{1:k}) \, \mathrm{d}\boldsymbol{y}_k \, \mathrm{d}\Theta \\
p(\Theta | \mathbf{z}_{1:k}) &= \int p(\boldsymbol{y}_k, \Theta | \mathbf{z}_{1:k}) \, \mathrm{d}\boldsymbol{y}_k \\
\boldsymbol{m}_{\Theta|\mathbf{z}_{1:k}} &= \int \Theta \, p(\Theta | \mathbf{z}_{1:k}) \mathrm{d}\Theta \\
\boldsymbol{\Sigma}_{\Theta|\mathbf{z}_{1:k}} &= \int (\Theta - \boldsymbol{m}_{\Theta|\mathbf{z}_{1:k}})(\Theta - \boldsymbol{m}_{\Theta|\mathbf{z}_{1:k}})^{\mathrm{t}} \, p(\Theta | \mathbf{z}_{1:k}) \, \mathrm{d}\Theta
\end{aligned}
\tag{11}
$$

The first three of these equations provide the solution to the problem of state estimation, while the last three provide solution to the problem of system identification. Here we employ an implicit Kalman filter for dynamic state estimation in conjunction with an adaptive metropolis algorithm [14] for parameter estimation, the detailed algorithm of which is outlined as follows:

Step 1: Input $\boldsymbol{\theta}_0 \sim p(\Theta)$,

For the sake of clarity, here, we mention the definition of the symbols Θ, and, $\boldsymbol{\theta}$. Here, Θ represents a random variable and $\boldsymbol{\theta}$ represents a realization of Θ.

Step 2: Run one state estimation algorithm for $\boldsymbol{\theta}_0$ using an implicit Kalman filter.

a. Initialization for implicit Kalman filter:

Input $\mathbf{P}_0^-(\boldsymbol{\theta}_0), \hat{\boldsymbol{y}}_0^-(\boldsymbol{\theta}_0), \mathbf{R}_0(\boldsymbol{\theta}_0), \mathbf{h}_0(\boldsymbol{\theta}_0), z_0, \boldsymbol{\Sigma}_{\boldsymbol{\nu}_0}, \bar{\mathbf{Q}}_0(\boldsymbol{\theta}_0), \boldsymbol{\Sigma}_{w_0}, \bar{\mathbf{F}}_0(\boldsymbol{\theta}_0), \bar{\boldsymbol{H}}_0(\boldsymbol{\theta}_0)$

b. For $k = 0, 1, \cdots N_T$

$$\mathbf{K}_k(\boldsymbol{\theta}_0) = \mathbf{P}_k^-(\boldsymbol{\theta}_0)\mathbf{h}_k^{\mathrm{t}}(\boldsymbol{\theta}_0)\left[\mathbf{R}_k(\boldsymbol{\theta}_0)\Sigma_{\boldsymbol{\nu}_k}\mathbf{R}_k^{\mathrm{t}}(\boldsymbol{\theta}_0) + \mathbf{h}_k(\boldsymbol{\theta}_0)\mathbf{P}_k^-(\boldsymbol{\theta}_0)\mathbf{h}_k^{\mathrm{t}}(\boldsymbol{\theta}_0)\right]^{-1}$$

$$\hat{\boldsymbol{y}}_k(\boldsymbol{\theta}_0) = \hat{\boldsymbol{y}}_k^-(\boldsymbol{\theta}_0) + \mathbf{K}_k(\boldsymbol{\theta}_0)\left(z_k - \mathbf{h}_k(\boldsymbol{\theta}_0)\hat{\boldsymbol{y}}_k^-(\boldsymbol{\theta}_0)\right)$$

$$\mathbf{P}_k(\boldsymbol{\theta}_0) = \left[\mathbf{I} - \mathbf{K}_k(\boldsymbol{\theta}_0)\mathbf{h}_k(\boldsymbol{\theta}_0)\right]\mathbf{P}_k^-(\boldsymbol{\theta}_0)$$

$$\hat{\boldsymbol{y}}_{k+1}^-(\boldsymbol{\theta}_0) = \bar{\mathbf{F}}_k(\boldsymbol{\theta}_0)\hat{\boldsymbol{y}}_k(\boldsymbol{\theta}_0) + \bar{\boldsymbol{H}}_k(\boldsymbol{\theta}_0)$$

$$\mathbf{P}_{k+1}^-(\boldsymbol{\theta}_0) = \bar{\mathbf{Q}}_k(\boldsymbol{\theta}_0)\Sigma_{\boldsymbol{w}_k}\bar{\mathbf{Q}}_k^{-\mathrm{t}}(\boldsymbol{\theta}_0) + \bar{\mathbf{F}}_k(\boldsymbol{\theta}_0)\mathbf{P}_k(\boldsymbol{\theta}_0)\bar{\mathbf{F}}_k^{\mathrm{t}}(\boldsymbol{\theta}_0)$$

$$I_2(\mathbf{z}_{1:k}, \boldsymbol{\theta}_0) = \mathbb{N}\left[\mathbf{z}_k : \mathbf{h}_k(\boldsymbol{\theta}_0)\hat{\boldsymbol{y}}_k^-(\boldsymbol{\theta}_0), \mathbf{R}_k(\boldsymbol{\theta}_0)\Sigma_{\boldsymbol{\nu}_k}\mathbf{R}_k^{\mathrm{t}}(\boldsymbol{\theta}_0) + \mathbf{h}_k(\boldsymbol{\theta}_0)\mathrm{P}_k^-(\boldsymbol{\theta}_0)\mathbf{h}_k^{\mathrm{t}}(\boldsymbol{\theta}_0)\right]$$

c. Compute $p\left(\boldsymbol{\theta}_0 \,|\mathbf{z}_{1:N_T}\right) = \mathbf{C}\, p(\boldsymbol{\theta}_0)\prod_{\alpha=1}^{N_T} I_2(\mathbf{z}_{1:\alpha}, \boldsymbol{\theta}_0)$

Step 3: Set $i = 1, \cdots N_p$, where N_p represents the sample size and input Σ_0, λ_0, $\bar{\alpha} = 0.234$.

Step 4: Compute $\mathbf{C}_i = \lambda_{i-1}\Sigma_{i-1}$. Draw $\hat{\boldsymbol{\theta}}^i \sim \mathrm{N}\left(\boldsymbol{\theta}_{i-1}, \mathbf{C}_i\right)$ and sample a uniform random variable $u \sim \mathrm{U}[0,1]$.

Step 5: Repeat step 2 for $\hat{\boldsymbol{\theta}}^i$ and compute $p\left(\hat{\boldsymbol{\theta}}^i \,|\mathbf{z}_{1:N_T}\right) = \mathbf{C}\, p\left(\hat{\boldsymbol{\theta}}^i\right)\prod_{\alpha=1}^{N_T} I_2\left(\mathbf{z}_{1:\alpha}, \hat{\boldsymbol{\theta}}^i\right)$.

Step 6: Compute the acceptance probability, $\alpha_i^{\mathrm{AM}} = \min\left[1, \dfrac{p\left(\hat{\boldsymbol{\theta}}^i \,|\mathbf{z}_{1:N_T}\right)}{p\left(\boldsymbol{\theta}_{i-1} \,|\mathbf{z}_{1:N_T}\right)}\right]$.

Step 7: If $u \le \alpha_i^{\mathrm{AM}}$, accept $\hat{\boldsymbol{\theta}}^i$ and set $\boldsymbol{\theta}_i = \hat{\boldsymbol{\theta}}^i$, otherwise reject $\hat{\boldsymbol{\theta}}^i$ and set $\boldsymbol{\theta}_i = \boldsymbol{\theta}_{i-1}$.

Step 8: Set $\boldsymbol{m}_{k|k}(\boldsymbol{\theta}_i) = \hat{\boldsymbol{y}}_k(\boldsymbol{\theta}_i); \bar{\Sigma}_{k|k}(\boldsymbol{\theta}_i) = \mathbf{P}_k(\boldsymbol{\theta}_i)$.

Step 9: Obtain a new estimate for the target covariance, $\Sigma_i = \mathrm{cov}\left(\boldsymbol{\theta}_0, \cdots \boldsymbol{\theta}_i\right)$.

Step 10: Compute $\gamma_i = i^{-\eta}, \eta \in (1/2, 1]$, the gain sequence.

Step 11: Compute $\log\lambda_i = \log\lambda_{i-1} + \gamma_i\left(\alpha_i^{\mathrm{AM}} - \bar{\alpha}\right)$.

Step 12: If $i \le N_p$, go to Step 4, else stop.

Step 13: Computation of moments of the state vector

a. $\boldsymbol{a}_{k|k} = \dfrac{1}{N_p}\sum_{i=1}^{N_p}\boldsymbol{m}_{k|k}(\boldsymbol{\theta}_i)$

b. $\boldsymbol{\Sigma}_{k|k} = \dfrac{1}{N_p}\sum_{i=1}^{N_p}\left[\bar{\Sigma}_{k|k}(\boldsymbol{\theta}_i) + \boldsymbol{m}_{k|k}(\boldsymbol{\theta}_i)\boldsymbol{m}_{k|k}^{\mathrm{t}}(\boldsymbol{\theta}_i)\right]$

In the above algorithm, steps 2 and 5 make use of the implicit Kalman filter for state estimation. While step 2 involves one run of implicit Kalman filter algorithm for the prior sample $\boldsymbol{\theta}_0$, step 5 involves N_p runs of state estimation algorithm for $\boldsymbol{\theta}_i, i = 1, \cdots N_p$. Thus, any computational gain offered by the implicit state estimation algorithm can result in a considerable gain in the combined state and parameter estimation problem of linear stiff systems.

5 NUMERICAL ILLUSTRATIONS

In this study, we consider a five-storied bending-torsion coupled building frame subject to El Centro ground acceleration (North-South component, recorded at Imperial valley station) [15]. The peak ground acceleration is scaled to a value of 0.12g. The frame is supported by four fixed base columns, out of which three columns are made of steel and one is of aluminum, resulting in stiffness asymmetry in the frame. Also, eccentric masses are placed on 1st, 2nd, 3rd, and 5th floor levels to simulate the effect of mass asymmetry in the response of the frame. The details of geometric dimensions, floor masses, cross-sectional properties, material properties, sensor locations, and applied ground motion can be found in an earlier study by the authors [5].

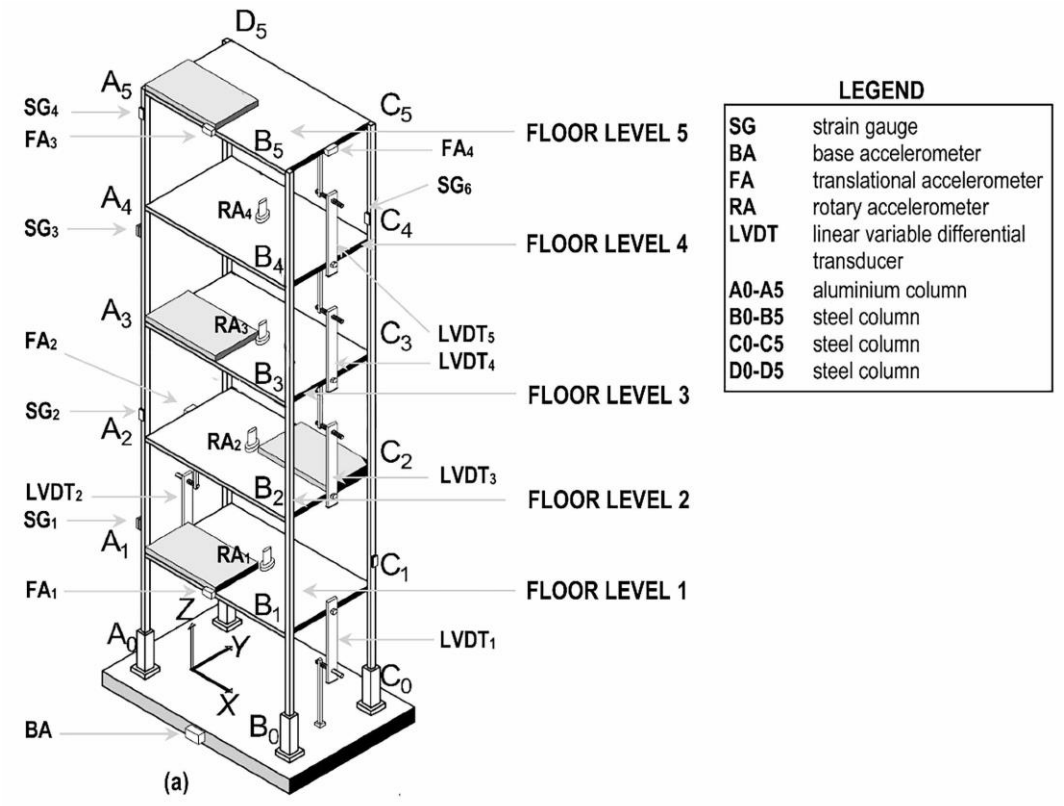

Figure 1. Experimental frame: sensor locations and types of sensors are indicated.

In the present study, we consider uncertainty in modeling the damping and column stiffnesses, while the floor masses are treated as deterministic quantities. Therefore, we have 15 damping ratios corresponding to 15 normal modes of vibrations and 20 stiffness parameters, considering each column stiffness in every story as a separate variable. We also consider the torsional stiffness of each floor due to the combined effect of all four columns, which results

in another 5 parameters for the overall frame. Thus, we have a total of 40 random variables for the stochastic response analysis of the frame. The random variables are arranged in a 40-dimensional random vector, $\boldsymbol{\Theta} = \left[k_1^1 \;\; k_2^1 \;\; k_3^1 \;\; k_4^1 \;\; k_\varphi^1 \;\; k_1^2 \;\; \ldots \;\; k_4^5 \;\; k_\varphi^5 \;\; \xi_1 \;\; \xi_2 \;\; \ldots \;\; \xi_{15} \right]^{\mathrm{t}}$. Here, the random variables, $k_1^j;\ 1 \le j \le 5$ denotes the story stiffnesses associated with aluminium column (marked as column A0-A5 in Figure 1), $k_2^j, k_3^j, k_4^j;\ 1 \le j \le 5$, are the story stiffnesses associated with steel columns (marked as column B0-B5, C0-C5, and, D0-D5 in Figure 1), $k_\varphi^j;\ 1 \le j \le 5$, are the torsional stiffnesses of j^{th} story, and ξ_r = damping ratio corresponding to r^{th} mode of vibration.

A stochastic response analysis is performed using 10000 samples of the vector random variable $\boldsymbol{\Theta}$, generated through Monte Carlo simulations. All the random variables denoting modal damping are assumed to be independent, whereas the random variables denoting the column stiffnesses within a story are considered to be dependent through a correlation coefficient matrix. The prior probability models and associated parameters for the system parameters are given in Table 1.

Table 1. Probability models for the parameters

Parameters	Probability distribution	Mean	COV
$k_1^j;\ 1 \le j \le 5$	Lognormal distribution	$6.0845 \times 10^4\ (\text{kN/m})$	0.05
$k_2^j, k_3^j, k_4^j;\ 1 \le j \le 5$	Lognormal distribution	$18.050 \times 10^4\ (\text{kN/m})$	0.05
$k_\varphi^j;\ 1 \le j \le 5$	Lognormal distribution	$0.7535 \times 10^4\ (\text{kNm/rad})$	0.05
$\xi_j; 1 \le j \le 15$	Lognormal distribution	0.04	0.10

The coefficients of correlations are taken as follows:

$$\rho\left(k_1^i, k_2^i\right) = 0.6,\ \rho\left(k_1^i, k_3^i\right) = 0.45,\ \rho\left(k_1^i, k_4^i\right) = 0.3,\ \rho\left(k_1^i, k_5^i\right) = 0.2,\ \rho\left(k_2^i, k_3^i\right) = 0.3,\ \rho\left(k_2^i, k_4^i\right) = 0.2,$$
$$\rho\left(k_2^i, k_5^i\right) = 0.1,\ \rho\left(k_3^i, k_4^i\right) = 0.2,\ \rho\left(k_3^i, k_5^i\right) = 0.1,\ \rho\left(k_4^i, k_5^i\right) = 0.5; i = 1, 2, \ldots, 5.$$
$$\rho\left(k_k^i, k_m^j\right) = 0;\ i \ne j;$$
$$\rho\left(\xi_i, \xi_j\right) = \delta_{ij};\ \delta_{ij} = \text{Kronecker's delta}$$

The performance of the building frame is assessed in terms of three performance measures, namely, PM_1, PM_2, and, PM_3, as discussed in section 2. As per prior response analysis, the average maximum inter-story drift is observed to be 0.14% of the story height and the average maximum inter-story rotation is found to be 0.0008 radians. The average base shear was recorded to be 19.27% of the weight of the building frame. In this study, for the calculation of PM_3, we take $c_1 = 0$ assuming the contribution of damping force is negligible towards maximum base shear, compared to the contribution of elastic restoring force.

The experimental frame is instrumented with 6 strain gauges, 5 uni-axial accelerometers, 4 rotary accelerometers, and 5 LVDTs (to measure inter-story drift), as shown in Figure 1. The arrangement for mounting LVDT consists of a combination of rigid wooden plank connected to the slab and a magnetic base that is anchored to the slab above. The applied base acceleration is also measured. The frame is mounted on a servo-hydraulic controlled, multi-axes, shake table that operates in a displacement-controlled mode. For the combined state and pa-

rameter estimation, eight sets of measurements are assimilated. These include inter-story drifts between the 1st and 2nd floor, 2nd and 3rd, 3rd and 4th floor, 4th and 5th floor, strain in aluminium columns in 1st and 3rd floor along x and y direction respectively, strain in steel columns in 2nd and 4th floor along y and x direction respectively. Using the combined state and parameter estimation algorithm, which is discussed in section 4, we obtain the posterior joint pdf of the parameters.

The estimated pdfs of the three performance measures, based on prior samples and posterior samples of the parameters are plotted in Figure 2. To compare the GRSI values observed based on prior responses and posterior responses, we select a common reference set A, for each response quantity of interest. The reference set, A, along with pdfs of prior and posterior responses are shown in Figure 2 (the interval between two dotted red lines indicates the set A).

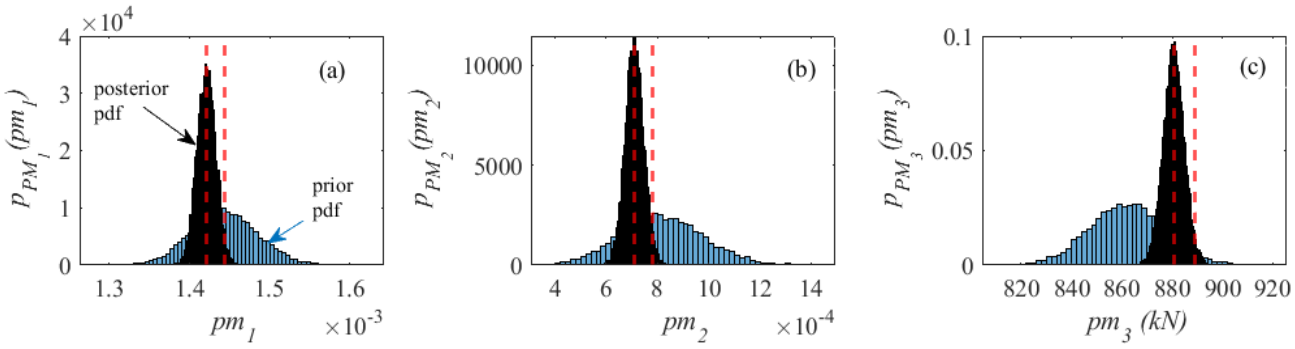

Figure 2. Pdfs of prior and posterior responses, (a) PM_1, reference set $A=[1.41,1.45]\times10^{-3}$ (b) PM_2, $A=[0.7110,0.7280]\times10^{-3}$, (c) PM_3, $A=[880,890]\,(\mathrm{kN})$

In this study, we consider three different grouping schemes of random variables for GRSA, as discussed below:

Case I. All the stiffness parameters associated with a particular story, are grouped together. Thus, we have five groups of random variables arising from the stiffness parameters of each story. This grouping scheme captures the effect of irregularity in stiffness distribution across different stories. We also derive three groups from the random variables pertaining to damping ratios, by collecting the damping ratios corresponding to 1st five natural modes into one group, similarly damping ratios corresponding to 6th through 10th normal modes, 11th through 15th normal modes into other two groups respectively. In summary, the groups of random variables are represented here as follows:

$$\boldsymbol{\Theta}=\left[\boldsymbol{\Theta}^1 \quad \boldsymbol{\Theta}^2 \quad \cdots \quad \boldsymbol{\Theta}^8\right]^{\mathrm{t}};$$

$$\boldsymbol{\Theta}^j=\left[k_1^j \quad k_2^j \quad k_3^j \quad k_4^j \quad k_\varphi^j\right];\ 1\le j\le 5,\ j=\text{story number},$$

$$\boldsymbol{\Theta}^6=\left[\xi_1 \quad \xi_2 \quad \cdots \quad \xi_5\right];\ \boldsymbol{\Theta}^7=\left[\xi_6 \quad \xi_7 \quad \cdots \quad \xi_{10}\right];\ \boldsymbol{\Theta}^8=\left[\xi_{11} \quad \xi_{12} \quad \cdots \quad \xi_{15}\right];$$

The results of GRSA based on prior pdfs and posterior pdfs of the parameters are plotted in Figures 3(a)-(c). The top three groups of random variables as per prior and posterior GRSA are reported in Table 2.

Case II. Here, the same 40 random variables are grouped into 8 groups following a different grouping scheme for the stiffness parameters. The stiffness parameters along a column line (in the vertical direction) are clubbed together to form a group, resulting in four groups. Another group is formed by collecting all the torsional stiffness parameters for all five stories. Three

other groups are formed from the damping ratios following the same scheme as discussed in case I. In this case, the groups of random variables are represented as follows:

$$\boldsymbol{\Theta} = \left[\boldsymbol{\Theta}^1 \quad \boldsymbol{\Theta}^2 \quad \cdots \quad \boldsymbol{\Theta}^8 \right]^t$$

$$\boldsymbol{\Theta}^j = \left[k_j^1 \quad k_j^2 \quad k_j^3 \quad k_j^4 \quad k_j^5 \right]; \quad 1 \le j \le 4, \; j = \text{ number of column line}$$

$$\boldsymbol{\Theta}^5 = \left[k_\varphi^1 \quad k_\varphi^2 \quad k_\varphi^3 \quad k_\varphi^4 \quad k_\varphi^5 \right]; \quad \boldsymbol{\Theta}^6, \boldsymbol{\Theta}^7, \text{and, } \boldsymbol{\Theta}^8 \text{ are the same as in Case I.}$$

The computed GRSI for prior and posterior models of the parameters are shown in Figures 4 (a)-(c). Top three important groups of random variables for the considered three performance measures are listed in Table 3.

Case III. Here, we compute the GRSI with respect to 40 individual random variables. The GRSI values are reported as *GRSI* (j); j =1, 2,…,40. Here, j is the number, that enumerates the position of the random variables in the vector $\boldsymbol{\Theta}$.

$$\boldsymbol{\Theta} = \left[k_1^1 \quad k_2^1 \quad k_3^1 \quad k_4^1 \quad k_\varphi^1 \quad k_1^2 \quad \ldots \quad k_4^5 \quad k_\varphi^5 \quad \xi_1 \quad \xi_2 \quad \ldots \quad \xi_{15} \right]^t$$

The results of GRSA for all three performance measures, with respect to individual parameters, based on their prior samples and posterior samples are compared in Figures 5(a)-5(c). All 40 random variables are ranked according to their relative importance measured through GRSI values, and the top 10 random variables are reported in Table 4.

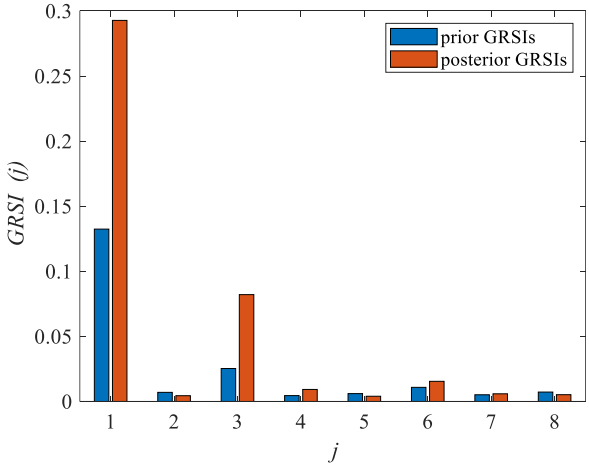

Figure 3 (a). Prior and posterior GRSI values for PM_1 in Case I

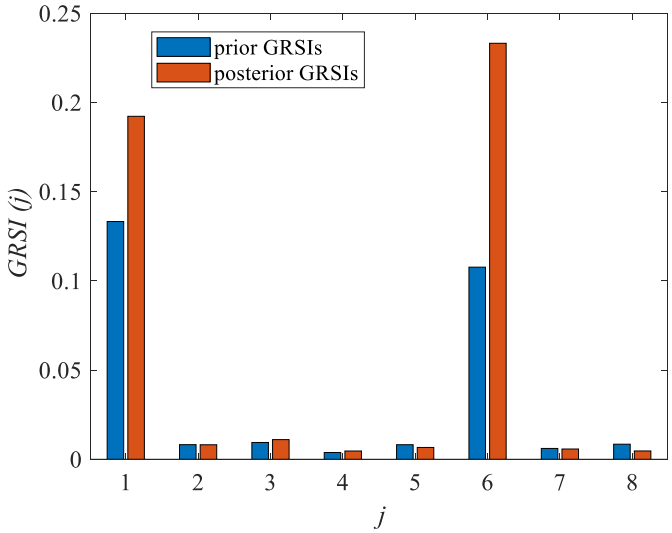

Figure 3 (b). Prior and posterior GRSI values for PM_2 in Case I

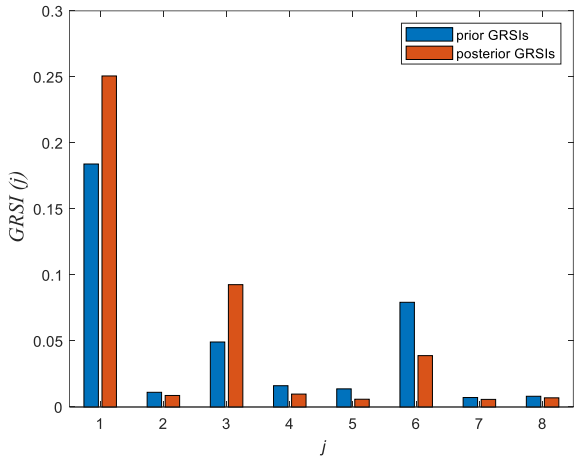

Figure 3 (c). Prior and posterior GRSI values for PM_3 in Case I

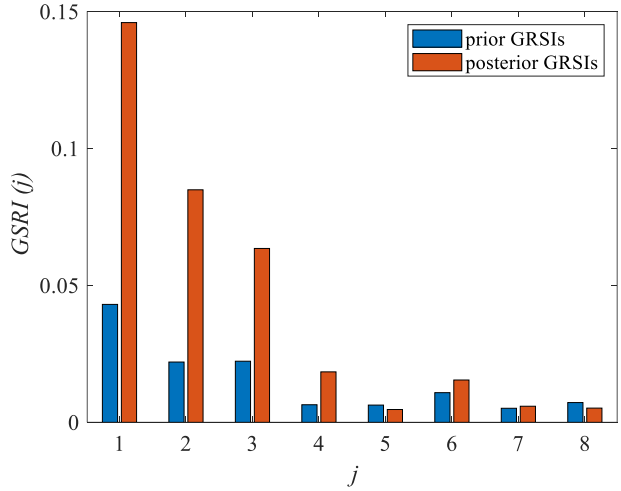

Figure 4 (a). Prior and posterior GRSI values for PM_1 in Case II

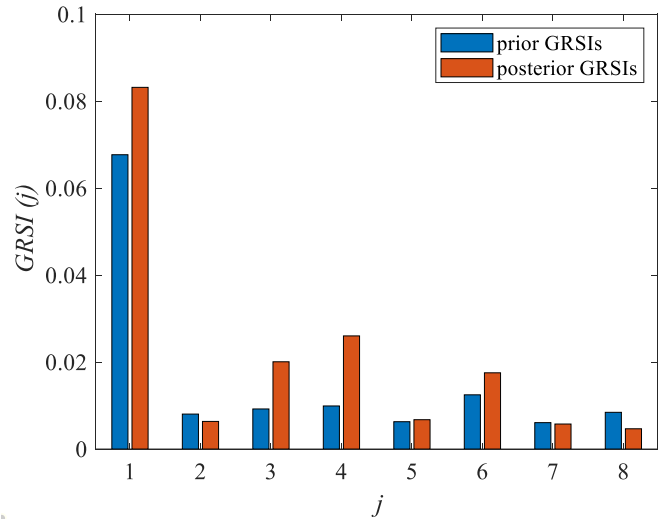

Figure 4 (b). Prior and posterior GRSI values for PM_2 in Case II

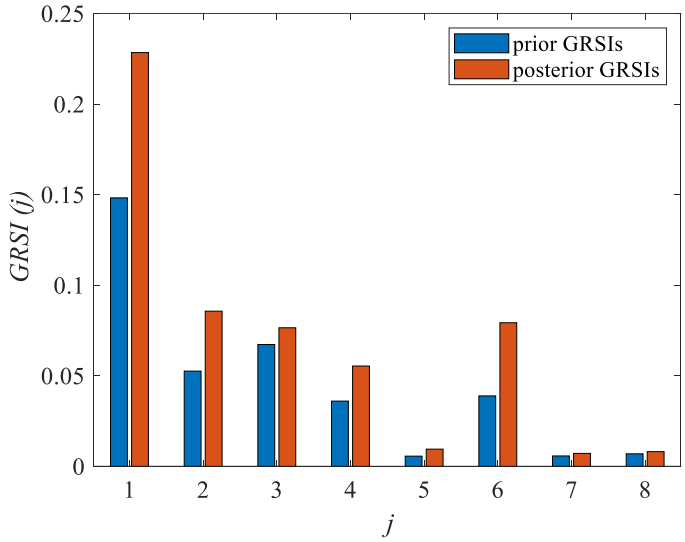

Figure 4 (c) Prior and posterior GRSI values for PM_3 in Case II

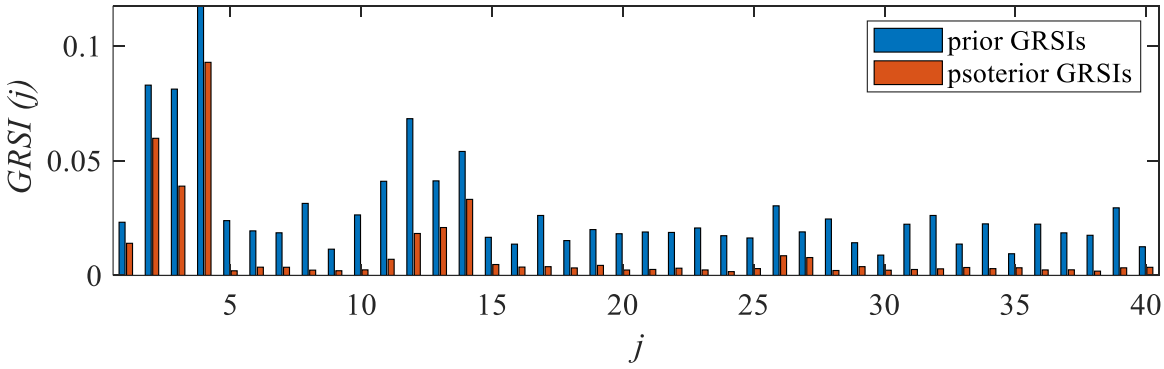

Figure 5 (a). Prior and posterior GRSI values for PM_1 in Case III

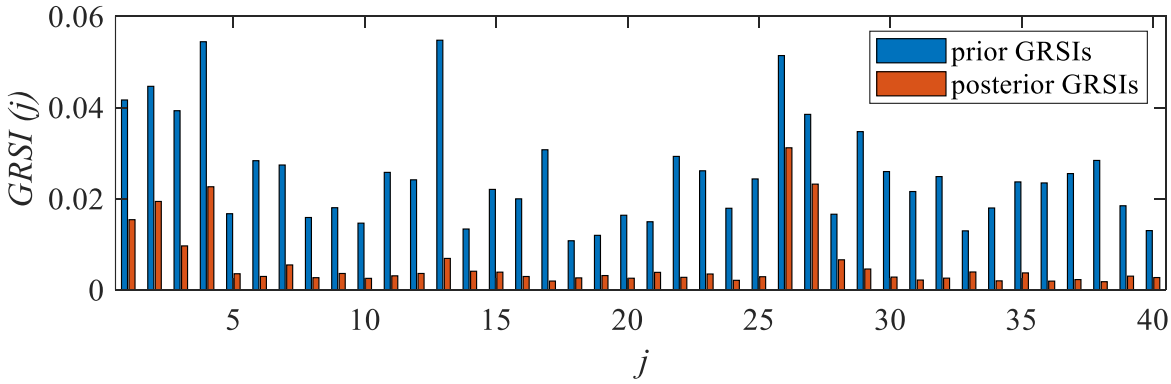

Figure 5 (b). Prior and posterior GRSI values for PM_2 in Case III

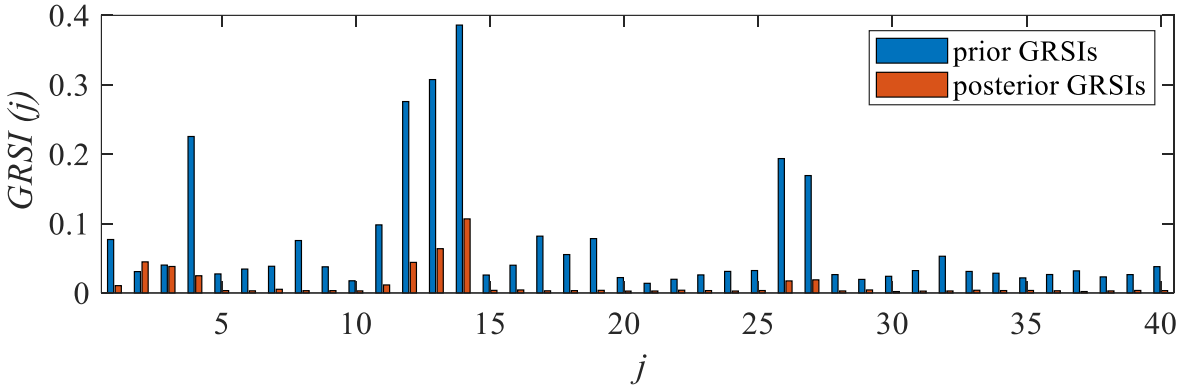

Figure 5 (c). Prior and posterior GRSI values for PM_3 in Case III

Table 2. Top three groups based on prior and posterior GRSI for case I

Performance Measures (PMs)	Top three groups based on Prior GRSI	Top three groups based Posterior GRSI
PM_1	1,3,6	1,3,6
PM_2	1,6,3	6,1,3
PM_3	1,6,3	1,3,6

Table 3. Top three groups based on prior and posterior GRSI for case II

Performance Measures (PMs)	Top three groups based on Prior GRSI	Top three groups based Posterior GRSI
PM_1	1,3,2	1,2,3
PM_2	1,6,4	1,4,3
PM_3	1,3,2	1,6,3

Table 4. Top 10 random variables based on prior and posterior GRSI for case III

Performance Measures (PMs)	Top ten random variables based on Prior GRSI	Top ten random variables based Posterior GRSI
PM_1	4,2,3,12,14,13,11,8,26,39	4,2,3,14,13,12,1,26,27,11

PM_2	26,27,13,4,2,1,3,29,17,22	26,27,4,2,1,3,13,28,7,29
PM_3	14,13,12,4,26,27,11,17,19,1	14,13,2,12,3,4,27,26,11,1

Based on the results shown in Figures 3-5, and, Tables 2-4, the following observations are made:

1. The GRSI values change significantly when they are calculated based on the posterior pdf of the parameters. This may lead to an alteration of the ranking of the parameters. In Table 2, we notice that the top three groups of random variables for PM_1 appear to be in the same order of importance in both prior and posterior GRSI-based rank ordering, although, there are significant differences in their prior and posterior GRSI values. For PM_2 and PM_3, the top three groups of random variables remain the same in both prior and posterior GRSA, but their order of importance changes. Considering all three *PM*s, we observe that the groups of random variables designated as 1,3 and, 6 are the most important in controlling the variability in the responses. Here, group 1 represents the combined stiffness of 1st story columns, group 3 represents the combined stiffness of 3rd story columns, and group 6 represents the set of damping ratios corresponding to 1st five normal modes of vibration.

2. In Table 3, we observe that the top three important groups of random variables remain the same as per prior and posterior GRSA (for the performance measure PM_1), but their order in ranking as per their relative importance changes. For PM_2, groups 1, 4, and 3 appear to be in the top three important groups as per posterior GRSA, whereas group 3 does not appear in the top three, while the ranking is done as per prior GRSA. A similar observation is made for PM_3.

3. In Table 4, we observe that, for the case of PM_1, 8 random variables are common in the lists of top ten random variables obtained in both prior and posterior GRSA. These random variables are designated by the numbers $\{2,3,4,11,12,13,14,26\}$. Also, it can be noticed that for the cases of PM_2, and, PM_3, 8 random variables appear in common to both the list of top ten random variables produced by prior and posterior GRSA. Three random variables designated by the numbers $\{4,13,26\}$ appear in all lists of the top ten random variables irrespective of prior or posterior GRSA. These three random variables represent the random variables $\{k_4^1, k_3^3, \xi_1\}$. Here, k_4^1, k_3^3 are 1st story and 3rd story column (steel column) stiffnesses respectively, and ξ_1 represents the damping ratio corresponding to 1st normal mode of vibration.

4. Based on prior GRSI values shown in Figures 5(a)-(b), we observe that the damping ratios corresponding to all 15 normal modes of vibration seem to be equally important, whereas posterior GRSI values suggest that only two modal damping ratios, corresponding to 1st and 2nd modes of vibration play a crucial role in producing variability in the responses PM_1, and PM_2 respectively. According to Figure 5(c), both prior and posterior GRSI values corroborate the fact, that modal damping associated with the first two modes governs the variability in the response PM_3.

5. Furthermore, it can be noticed in Figures 5(a)-(c), that posterior GRSA produces negligibly small GRSI values for the non-important random variables, whereas the GRSI values for the important random variables remain significantly large. Thus, posterior GRSA acts like a filter, that removes noises from the GRSI values and enhances the capability of classifying important and non-important random variables. Identifying the set of important and non-important random variables pertaining to an uncertain system helps in developing a model reduction scheme, where the response uncertainty is captured through a lesser number of random variables.

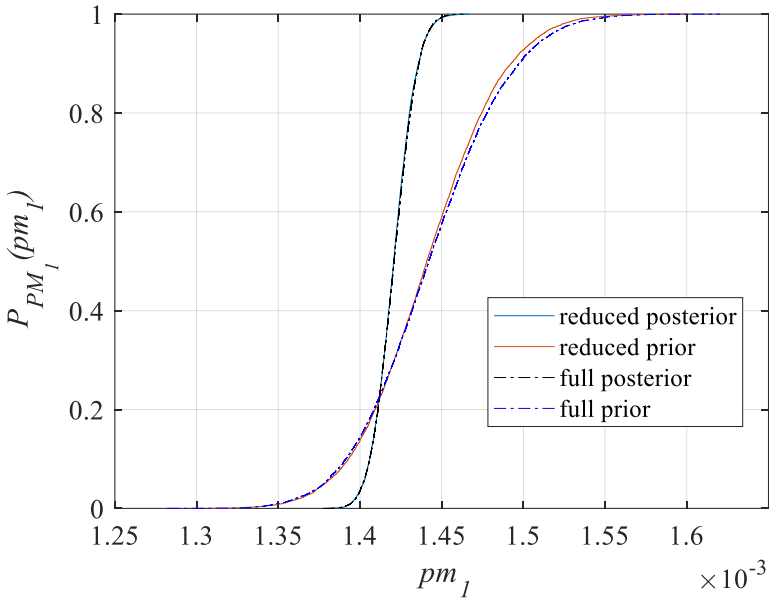

Figure 6. Estimation of CDFs of PM_1 for (a) reduced posterior model, (b) reduced prior model), (c)full posterior model, (d) full prior model. (Reduced models consider only the 10 topmost important random variables)

We also repeat the stochastic response analyses considering only the top 10 most important parameters as random variables, while the remaining parameters are treated as deterministic, setting their values to the specified mean values. We plot the CDF of the responses (here only results for PM_1 are shown in Figure 6) obtained based on reduced prior and posterior models and compared with the CDFs of the responses when all 40 parameters are considered as random variables. Thus, we achieve a meaningful model reduction (in terms of random variables). The CDFs of PM_1 for reduced and full model match well. Also, it is noted that the CDFs for the prior and posterior parameter models do not coincide, as the top 10 important random variables are different in these two cases, for a given parameter model (be it prior or posterior). Thus, GRSI values can play an important role in achieving model reduction.

6 CONCLUSIONS

This study focuses on updating GRSI values in an instrumented structure. We employ an MCMC sampler coupled with a recently developed implicit version of Kalman filter to estimate the parameter and states of a system simultaneously. Then, we perform GRSA by applying the factor mapping method on the converged parameter samples obtained in the combined parameter and state estimation step. It is observed that the GRSI values, thus ob-

tained based on the posterior parameter model, can be significantly different from the GRSI values achieved using the prior parameter model and this may lead to a difference in measuring the relative importance of the parameters and thus in rank order. The method has been applied to a five-storied bending-torsion coupled randomly parametered building frame (with uncertain parameters designated by 40 random variables). GRSA based on both prior and posterior samples of parameters was performed with respect to three performance measures, namely, maximum inter-story drift ratio, maximum inter-story rotation, and maximum base shear. The sets of important random variables or groups of random variables are identified, that govern the variability of the performance measures in a region of interest. It has been observed that the posterior GRSI values offer better means to classify the important and non-important random variables. The role of GRSI in stochastic model reduction is also studied.

REFERENCES

[1] Sobol, I. M. (2001). Global sensitivity indices for nonlinear mathematical models and their Monte Carlo estimates. Mathematics and computers in simulation, 55(1-3), 271-280.Probabilistic distance measure

[2] Greegar, G., & Manohar, C. S. (2015). Global response sensitivity analysis using probability distance measures and generalization of Sobol's analysis. Probabilistic engineering mechanics, 41, 21-33.

[3] Saltelli A, Tarantola S, Campolongo F, Ratto M. Sensitivity analysis in practice: a guide to assessing scientific models. vol. 1. Wiley Online Library; 2004.

[4] Saltelli A, Ratto M, Andres T, Campolongo F, Cariboni J, Gatelli D, et al. Global sensitivity analysis: the primer. John Wiley & Sons; 2008.

[5] Nisha, A., S., & Manohar, C., S. (2022). Dynamic state estimation in nonlinear stiff systems using implicit state space models. Struct Control Health Monitoring, 29(7): e2959. doi:10.1002/stc.2959.

[6] Paul, B., & Manohar, C. S. (2022). Factor mapping method for grouped input variables and its application to seismic damage analysis. Structural Safety, 97, 102214.

[7] Pardo L. Statistical inference based on divergence measures. CRC press; 2005.

[8] Bishop, C. M., & Nasrabadi, N. M. (2006). Pattern recognition and machine learning (Vol. 4, No. 4, p. 738). New York: springer.

[9] Der Kiureghian, A., & Liu, P. L. (1986). Structural reliability under incomplete probability information. Journal of Engineering Mechanics, 112(1), 85-104.

[10] Särkkä, S. (2013). Bayesian filtering and smoothing (No. 3). Cambridge university press, 2013.

[11] Joe, Harry. Dependence modeling with copulas. CRC press, 2014.

[12] Hyvärinen, Aapo, and Erkki Oja. Independent component analysis: algorithms and applications. Neural networks, 13.4-5: 411-430 (2000)

[13] Kloeden PE, Platen E. Numerical Solution of Stochastic Differential Equations. Springer; 2013:1-636.

[14] Luengo, D., Martino, L., Bugallo, M., Elvira, V., & Särkkä, S. (2020). A survey of Monte Carlo methods for parameter estimation. EURASIP Journal on Advances in Signal Processing, 2020(1), 1-62.

[15] https://peer.berkeley.edu/peer-strong-ground-motion-databases (last accessed in March 2021).